

## RESEARCH ARTICLE

# Impact of Antioxidants on DC and AC Electrical Properties of XLPE-Based Insulation Systems

**SIMONE VINCENZO SURACI** , (Member, IEEE),  
**DANIELE MARIANI**, (Graduate Student Member, IEEE),  
**AND DAVIDE FABIANI** , (Senior Member, IEEE)

Laboratory of Innovative Materials for Electrical Systems (LIMES), Department of Electrical Engineering, University of Bologna, 40136 Bologna, Italy

Corresponding author: Simone Vincenzo Suraci (simone.suraci@unibo.it)

This work was supported in part by the Euratom Research and Training Programme 2014–2018 under Grant 755183; and in part by the National Recovery and Resilience Plan (NRRP), Mission 04 Component 2 Investment 1.5 - NextGenerationEU, Call for tender n. 3277 dated 30/12/2021. Award Number: 0001052 dated 23/06/2022.

**ABSTRACT** In this article, the impact of two different antioxidants (Irganox®1076 and PS802) on the electrical properties of a cross-linked polyethylene (XLPE) matrix is investigated and discussed. Materials were tested by means of dielectric spectroscopy, thermally stimulated depolarization currents (TSDC) and DC conductivity measurements to provide a comprehensive analysis for their applications under AC and DC electric fields. Results reveal that electrical properties are notably modified by the introduction of additives and the amplitude of variation is somehow proportional to the concentration of the additive with respect to the polymer matrix. In particular, TSDC measurements claim that antioxidants introduce deep traps ( $>1$  eV) inside the base material and the density of these traps increases in accordance with antioxidant concentration. Moreover, due to the polar properties of these species, the complex permittivity raises with respect to base XLPE, and it adequately follows the antioxidant concentration. On the contrary, negligible variations in terms of DC conductivity are recorded.

**INDEX TERMS** XLPE, conductivity, permittivity, space charge, antioxidants, additives, additive traps.

## I. INTRODUCTION

During the last decades, the widespread diffusion of renewable energy plants with high installed power i.e., solar and wind farms in remote areas opened the issue of power transmission with high reliability throughout long distances.

In this sense, a proper design of the electrical apparatuses used for energy transmission, mainly cables and substation equipment, is a key step towards the desired target.

Given the characteristics of the power to be transmitted i.e., total transfer capability (TTC) and distances, the use of high voltage direct current (HVDC) cable systems is becoming more and more a common and viable solution. As a matter of fact, the recent advances in power electronics systems paved the way for the development of high reliable cost-effective converter stations employed to interface HVDC transmission systems with the traditional AC grid [1], [2].

The associate editor coordinating the review of this manuscript and approving it for publication was Guillaume Parent .

With reference to the cables, a lot of Research has been focusing on the development of innovative insulating materials for extruded HVDC cable applications conjointly with improved electrical properties i.e., low conductivity and reduced space charge accumulation [3], [4], [5], [6]. These characteristics are usually achievable by lowering the concentrations of impurities and contaminants inside the polymeric insulation. Indeed, all these species are often characterized by strong dipolar properties, and they can act as deep traps, affecting both the polarization and conduction mechanisms of the insulation. For example, if an electric field is applied, deep traps could yield the build-up of space charge. This may be a serious issue for the cable reliability, especially in HVDC systems. Despite the desirable purity, some additives e.g., antioxidants are required to prolong the lifespan of the primary insulation and, consequently, of the cable. It is worth noting that, even if the concentration of these additives is very limited inside polymeric systems for electrical applications [7], they may massively influence the electrical

characteristics of the insulation [8], [9], [10], [11]. In particular, typical concentrations of antioxidants inside polymers for HVDC insulations are usually  $\sim 0.2$  phr (per hundred resin). On the contrary, higher concentrations (up to 1.5 phr) are expected in the case of low voltage (LV) cables where the electrical insulation does not need excessive purity due to the low electric fields involved.

Polymers will change over time when exposed to heat, radiation, and other stresses e.g., electric fields or corrosive environments [12], [13], [14], [15]. These variations are a result of oxidative degradation reactions caused by radicals formed by the interaction of the surroundings with the organic matter. Antioxidants prevent deterioration mechanisms from occurring by undergoing a series of reactions widely reported in literature [16], [17]. Depending on the type of molecules the antioxidant reacts with, it is possible to distinguish between primary and secondary antioxidants.

Primary antioxidants are free-radical scavengers. They react with chain-propagating radicals e.g., peroxy, alkoxy and hydroxy radicals to form stable non-reactive species. The most used primary antioxidants are phenol-based. They are harnessed not only to ensure the stability of the insulating polymer during long-term thermal aging but also to guarantee a safe processing phase.

Secondary antioxidants are peroxide scavengers, and they are usually employed together with primary antioxidant in order to obtain a synergistic effect in preserving from oxidation degradation. The reaction scheme involving secondary antioxidant is mainly related to the decomposition of the hydroperoxides (ROOH), created as subproducts of the reaction of the primary antioxidants, into nonreactive species. For this reason, the secondary antioxidants are usually deployed inside the polymeric material along with a non-null concentration of primary antioxidants.

To date, quite extensive literature is present about the modification of the base polymeric matrix by means of the addition of antioxidant molecules [17], [18], [19], [20]. A vast majority of articles focuses on the physical-chemical characterization of the polymeric materials and how the antioxidants may efficiently delay the oxidation kinetics.

On the other hand, very little research [8], [9], [21], [22] discusses the effect of antioxidants on the electrical properties of the polymeric materials when deployed as primary insulation inside extruded cables.

Therefore, the aim of this article is to provide a broad analysis of the characteristics of the antioxidant species and their impact on the insulation electrical properties as a function of additive concentration. This is achieved providing:

- (i) *ab initio* calculation of the microscopical characteristics of the primary and secondary antioxidant molecules i.e., polarizability and dipolar momentum.
- (ii) Electrical experimental analyses under AC and DC electric fields. More specifically, the article presents the evolution of the most used electrical properties for cable design i.e., permittivity and DC conductivity, as a function of antioxidant type and concentration.

Additionally, the variations in terms of space charge accumulation are presented and discussed, in order to provide an insightful view of the use of antioxidant-filled materials as primary insulation for HVDC cable systems.

## II. MATERIALS AND METHODS

### A. MATERIALS

As primary insulation, silane crosslinked polyethylene (Si-XLPE) with different types and concentrations of antioxidants is used in this work. Samples were manufactured in the framework of the H2020 European Project “TeaM Cables” (team-cables.eu) and they are shown in Fig. 1. Irganox®1076 and Irganox® PS802 were employed in the polymeric mixture as primary and secondary antioxidant, respectively. Structural chemical formulas are shown in Fig. 2. Specifications of material compounds, along with the material index, are reported in Table 1. The thickness of the flat samples was  $\sim 500\mu\text{m}$ .

To ensure adequate electrode-specimen contact, gold electrodes were deposited on the sample surfaces through plasma cold sputtering. Geometries of gold electrodes were selected according to the requirements of the different testing setups. Before testing, metallized specimens were discharged for at least 24 hours.

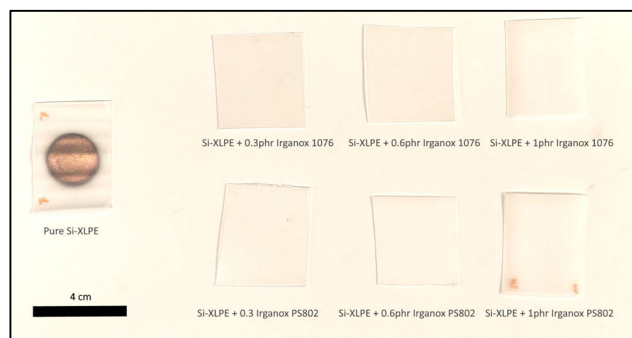


FIGURE 1. Photo of XLPE samples under test.

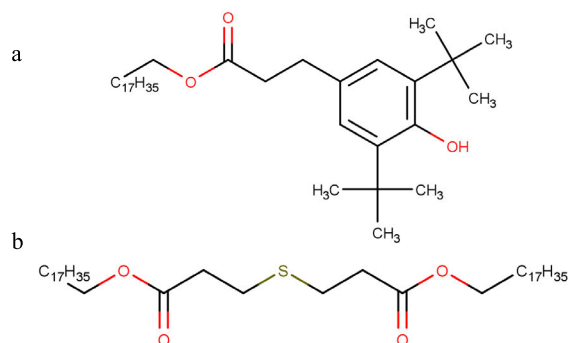


FIGURE 2. Structural chemical formula of (b) Irganox® 1076 and (c) Irganox® PS802.

**TABLE 1. Materials specifications. (phr – per hundred resin).**

Material index	Polymer matrix	Antioxidant type	Antioxidant concentration (phr)
0	Si-XLPE	-	0
1		Irganox® 1076	0.3
2			0.6
3			1
4		Irganox ® PS802	0.3
5			0.6
6	1		

### B. CHEMICAL SIMULATION SOFTWARE

Prior to experimental testing, antioxidant molecules were drawn inside the molecular simulation software (Chemaxon® MarvinSketch 21.8). The software allows the investigation of some of the most remarkable properties of the considered molecule (as in Fig. 2), including electrical ones.

From the simulation, it is possible to derive the displacement of charges throughout the molecule, along with the molecular polarizability and its permanent dipole moment. This latter rules the polarization mechanisms inside the polymer, e.g., modifying the material conductivity and permittivity at selected frequencies [10], [11], [21], [23], [24].

### C. DIELECTRIC SPECTROSCOPY

Complex permittivity of investigated materials was measured by means of a Novocontrol Alpha Dielectric Analyzer V2.2. Test settings were:

- Applied voltage:  $3 V_{rms}$
- Frequency:  $10^{-1}$ -  $10^6$ Hz
- Room temperature

Permittivity  $\hat{\epsilon}$  is a complex quantity defined as:

$$\hat{\epsilon} = \epsilon' - j\epsilon'' \quad (1)$$

where:  $\epsilon'$  is the real part of permittivity defined as the dielectric constant of the material and linked to the energy storable inside the dielectric;  $\epsilon''$  is the imaginary part of permittivity related to the dielectric losses of the material [25].

### D. DC CONDUCTIVITY

DC conductivity was measured according to the ASTM D257-14 (2021) standard. The standard requires the presence of a grounded guard electrode to get rid of the superficial current contribution to the registered current. In this way, the recorded current is only related to the current flowing through the bulk of the material, and it is related to the actual material conductivity. Nonetheless, the sensing area calculation considers part of the edge effects next to the signal electrode including the gap to the total diameter calculation. As a result, in this work, the sensing area was  $3.14 \text{ cm}^2$ .

Current flowing through the insulation was measured by means of a HVDC voltage generator (Keithley 2290E-5 5kV) and a picoamperemeter (Keysight B2981A). Values are acquired until the reaching of the steady-state value ( $i_{cond}$ )

or after 48h from the beginning of the test. The conductivity value is obtained through (2):

$$\sigma = \frac{J_c}{E} = \frac{i_{cond}/S}{E} \text{ (S/m)} \quad (2)$$

where  $J_c$  is the current density ( $\text{A/m}^2$ ),  $i_{cond}$  is the conduction current at the steady state (A),  $S$  is the sensing area ( $3.14 \text{ cm}^2$ ),  $E$  is the electric field (set equal to  $5 \text{ kV/mm}$  in this work).

### E. THERMALLY STIMULATED DEPolarIZATION CURRENT (TSDC)

#### 1) TSDC PROCEDURE AND SETUP

In a TSDC measurement, first the sample undergoes an isothermal polarization process [26], [27]. In particular, DC electric field ( $E=1 \text{ kV/mm}$ ) is applied by a Keithley 2290E-5, while the temperature is fixed at  $T_p=70^\circ\text{C}$ . The choice of this relatively low electric field is forced upon the limitations of the testing cell which does not allow to reach voltages above 1 kV. It is worth noting at this point that, due to problems related to the specimen, it was not possible to obtain reliable measurements in the case of material #6.

The conjoint application of these electric field and high temperature fosters charge injection from the electrodes to the insulator. Then, a cooling fluid (in this case liquid nitrogen, whose flow is controlled by a Novocontrol Novocool system, with an accuracy of  $0.1^\circ\text{C}$ ) decreases the temperature down to  $T_d=-50^\circ\text{C}$ . This is fundamental in order to dwindle the mobility of charge carriers inside the sample. Subsequently, after conduction regime has been reached, a depolarization phase takes place. Finally, a constant heating rate of  $\beta=3^\circ\text{C/min}$  is applied from  $-50$  to  $100^\circ\text{C}$ . This final step slowly unleashes all the charges which were previously trapped during the cooling volt-on phase. As a consequence, the TSDC measurement outcome, which is represented by the depolarization current density  $J$ , is measured by a Keysight B2981A picoamperemeter. The current measurement system was protected by a device made up of two diodes in antiparallel configuration in series to a  $1 \text{ M}\Omega$  resistor. A Novocontrol BDS1200 HV sample cell was employed, and its temperature was monitored by a Pt100 temperature probe. Its relationship with temperature leads to the two following results:

- The determination of the main trap depth inside the sample
- The calculation of the trap distribution, e.g., the trap density as a function of the trap depth

All steps regarding this data analysis are investigated in the following section and shown in Fig. 3.

#### 2) TRAP DEPTH COMPUTATION

This procedure is based upon the initial rise method, used among others by Mizutani et al. [28]. The principle is the following: the current density near the peak follows an Arrhenius behavior, at least for the low temperature tail.

In mathematical terms, this implies that:

$$J(T) = J_0 \cdot \exp\left(\frac{E_g}{k_B T}\right) \quad (3)$$

with  $J_0$  constant pre-exponential factor,  $E_g$  activation energy,  $k_B$  the Boltzmann constant. The activation energy found by TSDC measurements may be connected to polarization or detrapping processes. For this application,  $E_g$  can be considered as a trap depth, i.e., the energy which must be supplied to the insulating specimen in order to release the charge carriers. The theoretical justification for this assumption is given in Section IV.

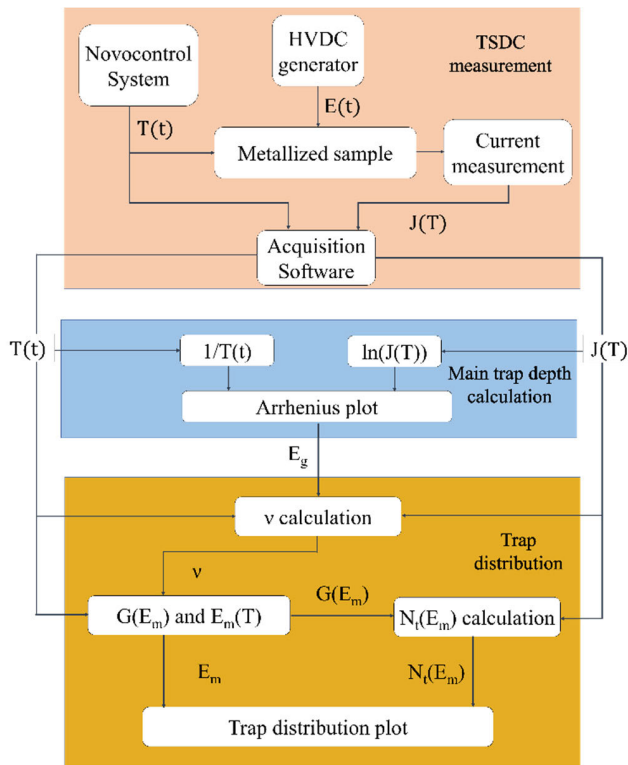


FIGURE 3. Schematics of data analysis for TSDC tests.

### 3) TRAP DISTRIBUTION COMPUTATION

Tian et al. [29] developed a model in order to find the trend of trap density with respect to trap depth, also called trap distribution, from the depolarization current data. To carry out this computation, it is necessary to consider the trap depth as belonging to a continuous spectrum of possible energy values  $E_m$ . In this way,  $E_g$  will be the particular value of trap depth with maximum trap density. This model requires the attempt-to-escape frequency  $\nu$ , a parameter which can be extracted from each peak of the plot from the following formula:

$$\nu = \frac{\beta E_g}{k_B T_M^2} \cdot e\left(\frac{E_g}{k_B T_M}\right) \quad (4)$$

where  $T_M$  is the temperature corresponding to the maximum of the peak and  $\beta$  is the constant heating rate.

At this point, it is possible to derive a correspondence between the spectra of temperature and trap depth by finding the value of  $E_m$  which maximizes the following function  $G(E_m, T)$  for each value of  $T$ :

$$G(E_m, T) = \nu e^{-\frac{E_m}{k_B T}} e^{-\frac{1}{\beta} \int_{T_0}^T \nu e^{-\frac{E_m}{k_B T}} dT} \quad (5)$$

Hence, the trap density,  $N_t$ , can be computed via:

$$f_0(E_m) N_t(E_m) = -\frac{2d}{el^2 G(E_m, T)} J(T) \quad (6)$$

where  $d$  is the sample thickness,  $e$  is the electron charge and  $l$  is the penetration distance traps of the injected charge (fixed at  $5 \mu\text{m}$  according to [29]), and it is assumed that the initial occupancy of the traps  $f_0(E_m)$  is equal to 1.

From each peak of the trap distribution, it is also possible to extract the trap volume density  $\rho$ , assuming they all resemble a symmetric distribution after the rising edge:

$$\rho = 2 \int_0^{E_g} N_t(E_m) dE_m \quad (7)$$

## III. RESULTS

### A. A-PRIORI SIMULATION RESULTS

As reported in Fig.2, the chemical structure of both the investigated antioxidants is characterized by the antioxidantizing group itself (i.e., phenolic and thioether groups) and one or more PE-like chains. The presence of these chains is important to obtain a good compatibility of the additive with the polymer matrix. The PE polymeric chain is characterized by apolar covalent bonds between C and H which result into non-localized charges with null dipolar moment (Table 2). On the other hand, the presence of the antioxidantizing groups significantly modifies this behavior leading to charge displacement (Fig. 4.a and 4.b) and a very high dipolar momentum ( $\sim 5$  D). The charge displacement is mainly localized on the high electronegative groups of the antioxidant i.e., next to the oxygen atoms. As a result, the molecule bends, providing a preferred direction to the dipole moment, which is usually oriented in the opposite direction of the oxygen (negative) group.

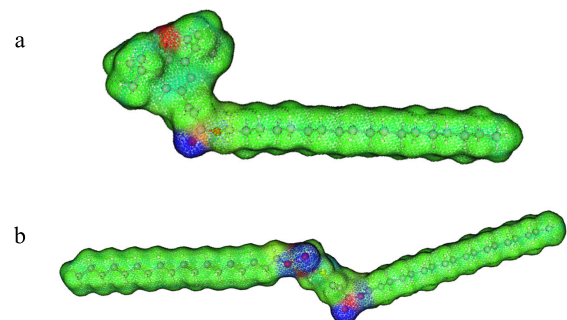


FIGURE 4. Charge displacement inside the antioxidant molecule (a) Irganox 1076 and (b) Irganox PS802.

TABLE 2. Chemical simulation results.

Species	Polarizability ( $\text{\AA}^3$ )	Dipole moment (D)
Pure PE	$\sim 2.4$ per $\text{CH}_2$	0
Irganox® 1076	70.51	4.99
Irganox ® PS802	93.95	4.47

The presence of these dipoles changes the response of the material to the electric field both in AC and DC. In particular, the polarization is usually enhanced in the presence of polar species due to the easier movement of these ignited by the action of the electric field. In the framework of a good insulating material, the polarization mechanisms have to be limited by abating the presence and formation of polar species at the lowest extent. Nonetheless, as reported in the introduction, some of these species, e.g., antioxidants, are necessary to guarantee a proper lifespan of the insulation in real condition to avoid the occurrence of oxidation reactions.

B. DIELECTRIC SPECTROSCOPY

The value of complex permittivity with frequency varies according to the molecular relaxation mechanisms occurring inside the material due to the application of an alternating electric field [25]. Consequently, the selection of the test frequency is a seminal step for proper analysis of the material.

The investigated frequency region is related to both dipolar and interfacial polarization [25], [30], [31]. By the application of an electric field with frequencies in the range of  $10^3$  to  $10^6$  Hz, long polymer chain characterized by a permanent dipole are expected to experience a relaxation, resulting into a peak in the imaginary part of permittivity. In a similar vein, for frequency lower than  $\sim 100$  Hz, response of interfaces inside the material, e.g., between the polymer matrix and the fillers, causes the raise of a relaxation peak. With reference to polyolefins, the base material is supposed not to exhibit significant dipolar momentum due to the apolarity of the macromolecules. Nonetheless, the response may vary due to the presence of polar additives.

For easier data analysis and comparison, it was chosen to report values of complex permittivity at two fixed frequencies i.e., 100 kHz and 0.1 Hz, which may be representative of the dipolar and interfacial polarization areas, respectively.

Figures 5 and 6 report the values of the real (a) and imaginary (b) part of permittivity for the two frequencies as a function of the antioxidant content inside the material.

It is seen that the addition of even little concentration of antioxidant leads to a surge of the real part of permittivity. The value of the dielectric constant for the materials with additives is then stabilized around an average value  $\sim 2.7$  for the primary antioxidant and  $\sim 2.6$  for the secondary antioxidant at high frequencies (Fig. 5.a), little variations are present and may be compared to the sensitivity of the instrumentation and/or specimen inhomogeneities. The same behavior can be underlined for the lowest frequency (Fig. 5.b) depicting slightly higher values ( $\sim 2.75$  and  $2.7$ , respectively).

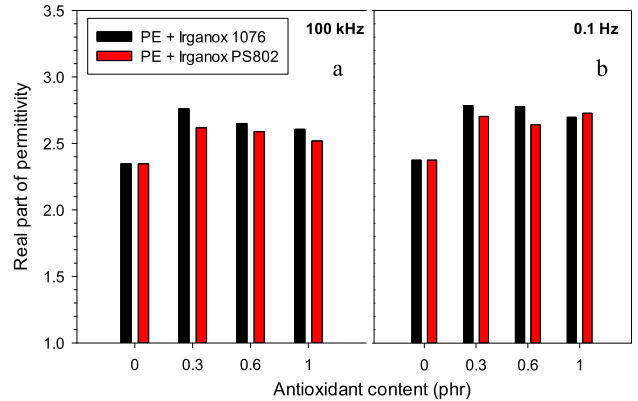


FIGURE 5. Real part of permittivity as a function of antioxidant contents at fixed frequencies (a) 100 kHz and (b) 0.1 Hz.

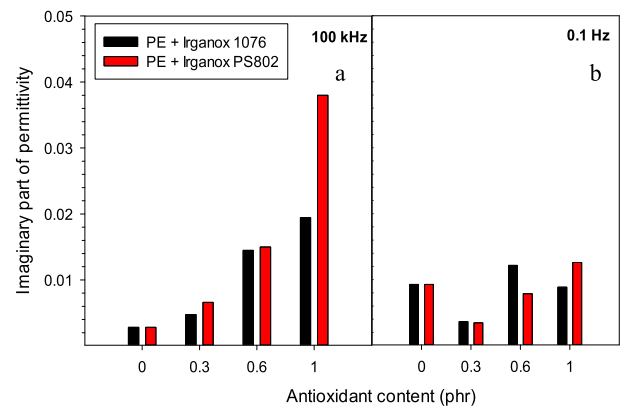


FIGURE 6. Imaginary part of permittivity as a function of antioxidant contents at fixed frequencies (a) 100 kHz and (b) 0.1 Hz.

The imaginary part of permittivity (Fig. 6) exhibits a different trend changing the testing frequency. As it may be seen from Fig. 6.a, the dielectric losses at high frequencies (100 kHz) manifest an exponential rise with the concentration of antioxidants. The values of dielectric losses for the two different antioxidants appear to be similar for concentrations  $\leq 0.6$  phr. The addition of antioxidants in higher concentration i.e., 1 phr exacerbates the dielectric losses in the case of the material with the secondary antioxidant while a more modest increase is recorded in the case of the primary antioxidant with the same concentration.

The trend of the imaginary part of permittivity shows another behavior in relation to the low frequencies (0.1 Hz). Here, the amplitude of the dielectric losses may not be directly linked to the type and concentration of antioxidant, due to a non-monotonic behavior. Nonetheless, the value of  $\epsilon''$  at 0.1 Hz for the neat material is higher than some other materials with additives. This suggests a different microstructural interfacial arrangement in the polymer matrix with the antioxidant addition.

C. DC CONDUCTIVITY RESULTS

Figure 7 reports the values of conductivity of the tested materials as a function of the antioxidant content. DC conductivity

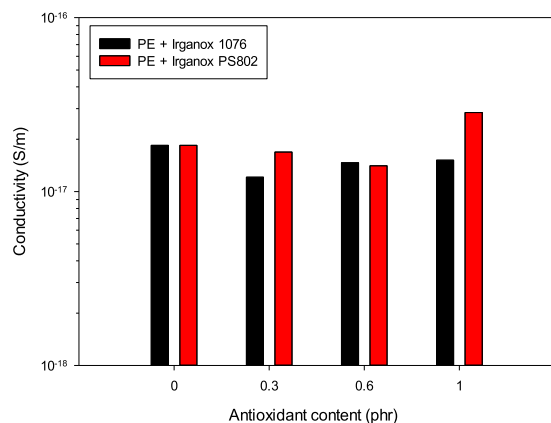


**FIGURE 7.** Charge displacement inside the antioxidant molecule (a) Irganox® 1076 and (b) Irganox® PS802.

seems to be negligibly modified among the different materials, recording values ranging from  $3 \cdot 10^{-17}$  and  $1 \cdot 10^{-17}$  S/m. Moreover, no monotonic variation of this quantity is measured as a function of the antioxidant concentration. For these reasons, the variation in the recorded values may be likely imputed to the different specimens used for tests rather than an actual modification of the property. Moreover, DC conductivity values are very similar to the ones reported in literature for Si-XLPE commercial materials, which usually own a small concentration of antioxidants in order to withstand the manufacturing process.

#### D. THERMALLY STIMULATED DEPolarIZATION CURRENT (TSDC)

##### 1) DEPolarIZATION CURRENT PLOTS

Depolarization current plots are shown in Fig. 8-9 for the primary and secondary antioxidant, respectively. Currents clearly show that incorporation of additives increases the intensity with respect to the neat sample. Moreover, an increasing content of Irganox®1076 and Irganox® PS802 leads to a further raise of the current. Another implication of the presence of antioxidants is a shift towards lower temperature values of the rising edge of the peaks. Nonetheless, the temperature corresponding to the peak for the two Irganox® PS802 composites was not significantly altered, whereas Irganox®1076 experienced a constant drop. A feature which can be extracted from the trends in Fig. 8-9 is that the low temperature tail slopes of the TSDCs of the composites become slightly steeper with antioxidant concentration. As a consequence, it can be surmised that the dominant trap depths, proportional to their slopes, will follow a similar behavior.

##### 2) TRAP DISTRIBUTION

The trap distribution plots (Fig. 10) show the trap density as a function of the trap depth. Such plots are obtained by applying Eq. 5-6 to the recorded depolarization currents (Figs. 8-9).

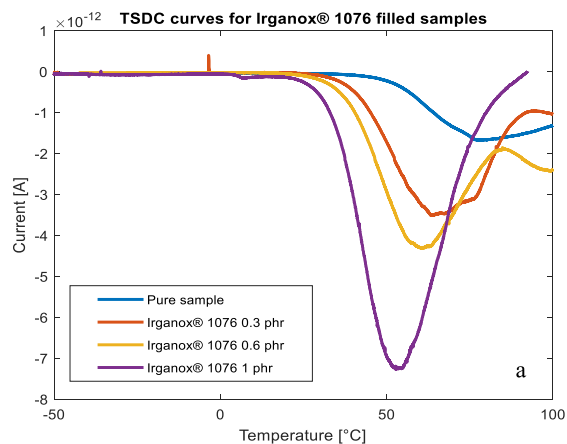


**FIGURE 8.** Depolarization current plots for Irganox® 1076 filled samples.

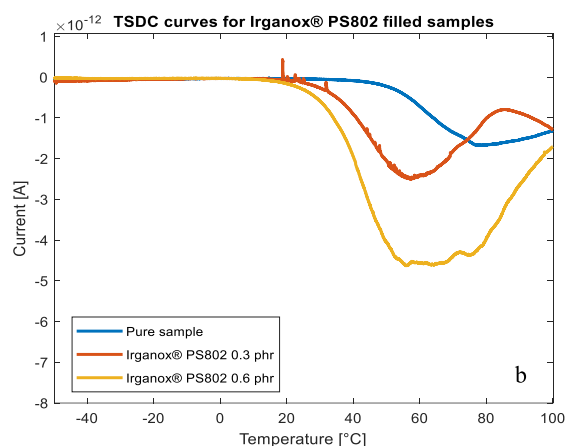


**FIGURE 9.** Depolarization current plots for Irganox® PS802 filled samples.

The peaks shown in Fig. 10 refer to the predominant traps present inside the material.

With reference to the pure XLPE material, the peak is centered at  $\sim 1$  eV which is already reported in literature as a typical value for this kind of material [32], [33]. The introduction of antioxidants causes the shift of the main trap peak towards higher trap depths ( $\sim 1.4$  and  $\sim 1.2$  for the primary and secondary antioxidant, respectively). The prevalent trap depth value is not constant, but it slightly increases as the content of antioxidant grows (Fig. 11). The tentative underpinning reason for this behavior is provided in the *Discussion Section*.

Additionally, as the antioxidant concentration raises, the peaks heighten and expand, suggesting a higher number of traps with more diverse depths. Finally, it is possible to quantify the number of traps per unit volume (Fig. 12) by integrating the trap distribution peak (Eq. 7). Consistently, the number of traps increases with the antioxidant concentration, implying the appropriateness of this technique for quantitative analyses. The values obtained by the analyses of the TSDCs are also displayed in Table 3.

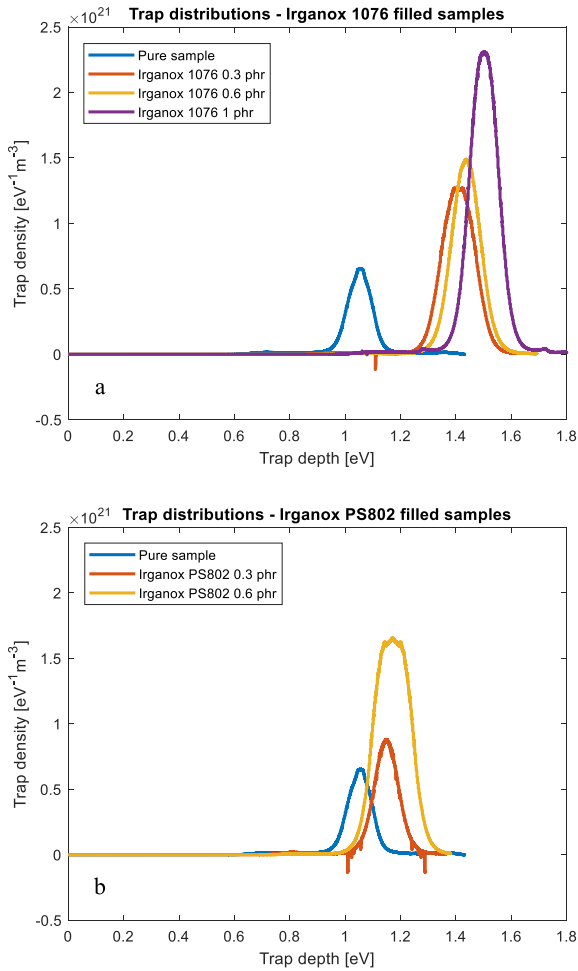


FIGURE 10. Trap distribution for the (a) Irganox® 1076 and (b) Irganox® PS802 filled materials.

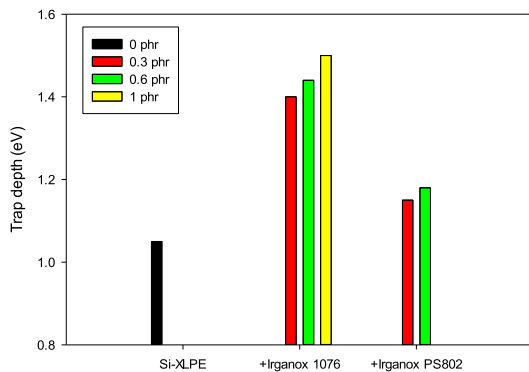


FIGURE 11. Trap depth evolution as a function of the additive concentration for the material under test.

IV. DISCUSSION

Results reported in the previous section demonstrated how inside a highly pure material, like the reference one in this work, even a little concentration of antioxidants may influence the material electrical properties. The reason for that has to be found in the dipolar and charge trapping properties of

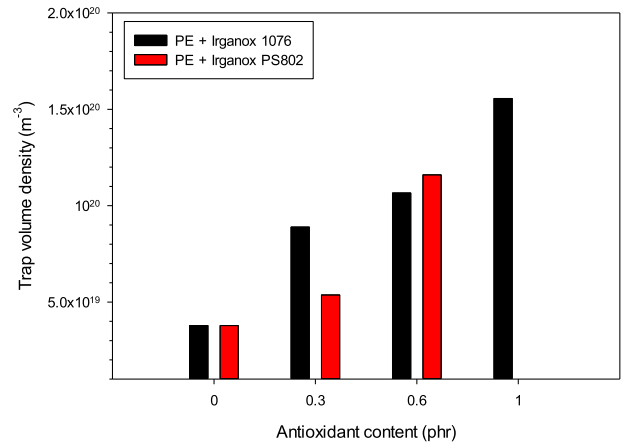


FIGURE 12. Trap volume densities for all the samples.

TABLE 3. Trap distribution data.

Material index	Main trap depth (eV)	Max value for trap density ( $\text{eV}^{-1} \text{m}^{-3}$ )	Trap volume density ( $\text{m}^{-3}$ )
1	1.05	$5.9 \cdot 10^{20}$	$3.78 \cdot 10^{19}$
2	1.4	$1.26 \cdot 10^{21}$	$8.89 \cdot 10^{19}$
3	1.44	$1.48 \cdot 10^{21}$	$1.06 \cdot 10^{20}$
4	1.5	$2.3 \cdot 10^{21}$	$1.56 \cdot 10^{20}$
5	1.15	$8.73 \cdot 10^{20}$	$5.37 \cdot 10^{19}$
6	1.18	$1.64 \cdot 10^{21}$	$1.16 \cdot 10^{20}$

these molecules as seen in the chemical simulations shown in Section III-A. As known, the presence of dipoles affects the distribution of the electrical field inside the material, both in AC and DC. Nonetheless, as discussed above, antioxidants are required to ensure protection against degradation and a proper lifespan of the equipment. All this being said, it is evident how maintaining of the concentration of these species at sufficiently low values is a very important issue to be properly addressed during the manufacturing, design and application phase of insulated power cables. In particular, it is worth recalling that during the life of HVDC cables, transient AC electric fields may be superimposed to the DC electric field also in HVDC cable systems during maneuvers, impulses and polarity reversals. For this reason, the understanding on the impact of these additives on the insulating material throughout all the phases of the HVDC cable system is crucially important to ensure a correct application life of these cables.

Focusing on the AC properties, antioxidant molecules show to modify the complex permittivity depending on the testing frequency. With reference to the real part of permittivity, the influence of frequency is really modest (Fig. 5), but one can notice a clear separation between the neat material and the ones with additives which depicts higher values of the electrical property.

Given the polar nature of the additives used in this article, their dielectric relaxation is supposed to occur in the highest frequency region of the considered range. According to Debye’s model and confirmed by various works [15], [25], [34], [35], the relaxation peak related to

the dipolar polarization mechanism is seen in the imaginary part of permittivity at  $\sim 10^5$  Hz. Indeed, Figure 6.a confirms this assumption showing the value of  $\epsilon''$  at 100 kHz to exponentially increase with the concentration of additives. In particular, despite the different absolute values of the dielectric losses caused by the distinct dipolar properties (Table 2) of the two antioxidants, the imaginary part of permittivity (Fig. 6) depicts very good correlation between the additive amount and the electrical property.

The polarity of the included species influences, with a different extent, also the DC properties of the base material. In particular, while the antioxidant content has negligible impact on the DC conductivity (Fig. 7), it notably alters the trend of the related TSDCs (Fig. 8-9).

As far as depolarization current is concerned, when activation energy increases, a rise in the corresponding peak temperature is expected. On the other hand, experimental results seem not to follow this general indication. This can be deduced from Table 3 and Fig. 8-10, which show that, while activation energy increases with antioxidant content, the peak temperature experiences a constant drop. A possible explanation for this behavior may lie in the findings of a previous work [36], which suggests that antioxidant crystals could undergo a melting process at  $\sim 50^\circ\text{C}$ . Thus, this phenomenon might have an influence on the position of the TSDC peaks with increasing antioxidant content, gradually shifting them from  $\sim 70^\circ\text{C}$  of the pure specimen towards  $\sim 50^\circ\text{C}$ .

As known [37], [38], [39], the TSDCs may provide information on both the polarization relaxation and de-trapping (space charge) mechanisms. Distinguishing between the two is particularly challenging if no additional tests or *a-priori* analyses are performed on the same materials. In particular, the main polymer matrix here used (polyethylene), is found to own various polarization mechanisms, namely:  $\alpha$ ,  $\beta$  and  $\gamma$  relaxations [37]. These relaxations are characterized by different types of motions, caused by the electric field, of various molecular structures. Moreover, different activation energies are usually ascribed to the different relaxations. With reference to the mathematical data treatment reported in Section II, the obtained values ( $>1$  eV) may be linked to the  $\alpha$ -relaxation mechanisms, associated to processes in the crystalline region. Despite the same polymeric matrix, these values change among the different materials under test, discarding the hypothesis. In addition, the antioxidants are commonly placed in the amorphous region, providing no contribution to the  $\alpha$ -relaxation of the polyethylene.

Furthermore, additives, especially antioxidants, are reported in literature [10], [11], [33], [40] to act as *chemical deep traps* inside the polymeric material. These traps are characterized by depth  $> 1$  eV and, if in high concentrations, they may be a concern due to the related space charge accumulation.

All this being said, it is evident how the values obtained by the analyses of the TSDCs (Fig. 10-12) may be directly imputed to the trapping properties of the materials.

Though one would expect that the base polyethylene would own just shallow traps caused by e.g., little interfaces between the crystalline and amorphous region of the polymer, it is reported, in Section III-D, that some traps with depth of  $\sim 1$  eV are also present. This is also seen in works by other authors [10], [11], [32], [33], who impute these traps to the intrinsic defects which are present in polyethylene. Even though the depth is quite high, it is still lower than that of deep traps created by other chemical groups e.g., antioxidants. Indeed, experimental results reported in Section III exhibit a shift towards higher depths of the trap distribution for materials with additives. The two different antioxidants introduce different traps to the base material and the amplitude of the trap density peak is directly proportional to the concentration of the additives. In particular, the primary antioxidant (Irganox® 1076) depicts the highest trap depth ( $>1.4$  eV) while shallower traps ( $\sim 1.2$  eV) are related to the secondary antioxidant (Irganox® PS802). The former trap depth is in agreement with DFT (Density functional Theory) calculations on phenolic antioxidants performed in [33], which results in a value of  $\sim 1.5$  eV by combing the electron affinities of the neat and filled materials.

It is worth noting how the trap depth slightly increases as a function of the concentration (Fig. 11). The reason for that may be found in the diverse interaction of the additives with the electric field when they are present in different contents. This behavior might be ascribed to the presence of interchain electron states [41]. As reported in [41], electrons creating space charge are not uniformly distributed at the microscopic level due to local inhomogeneities in the density of PE. In particular, electrons tend to accumulate where the density is lower e.g., at the interfaces. The introduction of additives also distorts the structural arrangement of the polymer matrix, usually leading to a reduction of crystallinity ratio and, consequently, of the density of the resulting material. This implies that the main trap peak (Fig. 11) is not only related to the presence of the chemical species itself (which would introduce in the material traps characterized by a unique trap depth) but also to the resulting additional interfacial areas and reduced local PE density which enhance electron trapping. As a result, as we consider higher concentration of the additive, the peak related to the main trap inside the material shifts towards higher trap depths as seen in Fig. 11. Moreover, the number of traps per unit volume, hence the trap volume density (Fig. 12), increases as the concentration of antioxidants grows.

Similar reasoning is also seen in [33], where the authors simulated the response of an antioxidant molecule both outside and inside a PE matrix. In the work, it is seen how the electron affinity of the antioxidant raises when placed in a PE matrix rather than *stand alone*.

Eventually, even considering some possible limitations arising from the theoretical assumption underpinning TSDC analysis, namely full trap occupancy, it is evident how electrical properties (i.e., imaginary part of permittivity at high frequency and trap density derived from TSDCs) are

modified by the additive content. Therefore, they may represent possible indicators of the additive content inside the material, even if additives are present in very low amount.

## V. CONCLUSION

This work focused on the experimental analysis of the change in the electrical properties of XLPE insulated materials by the addition of different types and concentrations of antioxidants. Results show that, despite different absolute values, the trend of the electrical properties as a function of additive concentration is similar between the primary and secondary antioxidants. The alteration of the properties is mainly related to the polar properties of these additives. In particular, the dielectric losses at high frequencies ( $\sim 10^5$  Hz) adequately follow the concentration of the additives, exhibiting an exponential increase of  $\varepsilon''$  as a function of additive concentrations.

With reference to the DC properties of the material, despite very limited differences in terms of conductivity, the introduction of antioxidants to the polymer matrix deeply modifies the space charge properties of the material. In particular, it was reported that the main trap depth of base material ( $\sim 1$  eV) is raised to 1.2 and 1.4 due to the addition of the primary and secondary antioxidant, respectively. The depth of the main traps introduced is not constant with the concentration of the additives, but it slightly intensifies. This peculiar behavior was imputed to the presence of interchain electron states created by additional interfaces and variation in local material density.

Eventually, the results reported in this work suggest that the used electrical techniques may be suitable as a quantitative assessment of the additive and other polar species concentration inside polymers. For this reason, future work on this topic will include the use of dielectric spectroscopy and TSDC analyses for the estimation of the aging level of the insulating material. This would envisage the use of these techniques as nondestructive condition monitoring techniques (NDTs) in relevant environments.

## ACKNOWLEDGMENT

This publication reflects only the authors' view, and the European commission is not responsible for any use that may be made of the information it contains.

## REFERENCES

- [1] D. van Hertem, O. Gomis-Bellmunt, and J. Liang, *HVDC Grids: For Offshore and Supergrid of the Future*. Hoboken, NJ, USA: Wiley, 2016.
- [2] A. Viatkin, M. Ricco, R. Mandrioli, T. Kerekes, R. Teodorescu, and G. Grandi, "Sensorless current balancing control for interleaved half-bridge submodules in modular multilevel converters," *IEEE Trans. Ind. Electron.*, vol. 70, no. 1, pp. 5–16, Jan. 2023, doi: [10.1109/TIE.2022.3156035](https://doi.org/10.1109/TIE.2022.3156035).
- [3] X. He, I. Rytöluoto, P. Seri, R. Anyszka, A. Mahtabani, H. Naderiallaf, M. Niittymäki, E. Saarimäki, C. Mazel, G. Perego, K. Lahti, M. Paajanen, W. Dierkes, and A. Blume, "PP/PP-HI/silica nanocomposites for HVDC cable insulation: Are silica clusters beneficial for space charge accumulation?" *Polym. Test.*, vol. 98, Jun. 2021, Art. no. 107186, doi: [10.1016/j.polymertesting.2021.107186](https://doi.org/10.1016/j.polymertesting.2021.107186).
- [4] T. Andritsch, A. Vaughan, and G. C. Stevens, "Novel insulation materials for high voltage cable systems," *IEEE Elect. Insul. Mag.*, vol. 33, no. 4, pp. 27–33, Jul. 2017, doi: [10.1109/MEL.2017.7956630](https://doi.org/10.1109/MEL.2017.7956630).
- [5] M.-L. Locatelli, C. D. Pham, S. Diahm, L. Berquez, D. Marty-Dessus, and G. Teyssède, "Space charge formation in polyimide films and polyimide/SiO<sub>2</sub> double-layer measured by LIMM," *IEEE Trans. Dielectr. Electr. Insul.*, vol. 24, no. 2, pp. 1220–1228, Apr. 2017, doi: [10.1109/TDEI.2017.006172](https://doi.org/10.1109/TDEI.2017.006172).
- [6] Z. Lei, D. Fabiani, F. Palmieri, C. Li, T. Han, G. Selleri, F. Grolli, M. Speranza, and S. V. Suraci, "Space charge characteristics of XLPE and semiconductive layer coated with graphene," *IEEE Trans. Dielectr. Electr. Insul.*, vol. 27, no. 1, pp. 128–131, Feb. 2020, doi: [10.1109/TDEI.2019.008347](https://doi.org/10.1109/TDEI.2019.008347).
- [7] G. Mazzanti, J. Castellon, G. Chen, J. C. Fothergill, M. Fu, N. Hozumi, J. H. Lee, J. Li, M. Marzinotto, F. Mauseth, P. Morshuis, C. Reed, I. Troia, A. Tzimas, and K. Wu, "The insulation of HVDC extruded cable system joints. Part 1: Review of materials, design and testing procedures," *IEEE Trans. Dielectr. Electr. Insul.*, vol. 26, no. 3, pp. 964–972, Jun. 2019, doi: [10.1109/TDEI.2019.007916](https://doi.org/10.1109/TDEI.2019.007916).
- [8] S. V. Suraci, C. Spinazzola, and D. Fabiani, "Analysis on the impact of additives on space charge behavior of thermally aged XLPE plaques," in *Proc. IEEE Conf. Electr. Insul. Dielectric Phenomena (CEIDP)*, Denver, CO, USA, Oct. 2022, pp. 41–44.
- [9] D. Mariani, S. V. Suraci, and D. Fabiani, "Impact of additives and fillers on space charge behavior of polyethylene insulation: Investigation and modeling," in *Proc. IEEE 4th Int. Conf. Dielectr. (ICD)*, Jul. 2022, pp. 62–65, doi: [10.1109/ICD53806.2022.9863554](https://doi.org/10.1109/ICD53806.2022.9863554).
- [10] M. Unge, C. Törnkvist, and T. Christen, "Space charges and deep traps in polyethylene—Ab initio simulations of chemical impurities and defects," in *Proc. IEEE Int. Conf. Solid Dielectr. (ICSD)*, Jun. 2013, pp. 935–939, doi: [10.1109/ICSD.2013.6619874](https://doi.org/10.1109/ICSD.2013.6619874).
- [11] M. Meunier, N. Quirke, and A. Aslanides, "Molecular modeling of electron traps in polymer insulators: Chemical defects and impurities," *J. Chem. Phys.*, vol. 115, no. 6, pp. 2876–2881, Aug. 2001, doi: [10.1063/1.1385160](https://doi.org/10.1063/1.1385160).
- [12] M. Celina, K. T. Gillen, and R. A. Assink, "Accelerated aging and lifetime prediction: Review of non-arrhenius behaviour due to two competing processes," *Polym. Degradation Stability*, vol. 90, no. 3, pp. 395–404, Dec. 2005, doi: [10.1016/j.polymdegradstab.2005.05.004](https://doi.org/10.1016/j.polymdegradstab.2005.05.004).
- [13] X. Colin, "Humid and thermal oxidative ageing of radiation cured polymers—A brief overview," *Frontiers Chem.*, vol. 9, Jan. 2022, Art. no. 797335, doi: [10.3389/fchem.2021.797335](https://doi.org/10.3389/fchem.2021.797335).
- [14] B. Fayolle, E. Richaud, X. Colin, and J. Verdu, "Review: Degradation-induced embrittlement in semi-crystalline polymers having their amorphous phase in rubbery state," *J. Mater. Sci.*, vol. 43, no. 22, pp. 6999–7012, Nov. 2008, doi: [10.1007/s10853-008-3005-3](https://doi.org/10.1007/s10853-008-3005-3).
- [15] S. Hettal, S. V. Suraci, S. Roland, D. Fabiani, and X. Colin, "Towards a kinetic modeling of the changes in the electrical properties of cable insulation during radio-thermal ageing in nuclear power plants. Application to silane-crosslinked polyethylene," *Polymers*, vol. 13, no. 24, p. 4427, Dec. 2021, doi: [10.3390/polym13244427](https://doi.org/10.3390/polym13244427).
- [16] C. Armstrong, M. A. Plant, and G. Scott, "Mechanisms of antioxidant action: The nature of the redox behaviour of thiodipropionate esters in polypropylene," *Eur. Polym. J.*, vol. 11, no. 2, pp. 161–167, Feb. 1975, doi: [10.1016/0014-3057\(75\)90141-X](https://doi.org/10.1016/0014-3057(75)90141-X).
- [17] B. Kirschweg, D. Tátraaljai, E. Földes, and B. Pukánszky, "Natural antioxidants as stabilizers for polymers," *Polym. Degradation Stability*, vol. 145, pp. 25–40, Nov. 2017, doi: [10.1016/j.polymdegradstab.2017.07.012](https://doi.org/10.1016/j.polymdegradstab.2017.07.012).
- [18] Y. Zheng, Y. Long, D. Yi, H. Zhang, J. Gao, K. Wu, and J. Li, "Correlation between antioxidant depletion kinetic model and ageing behaviour of cross-linked polyethylene cable insulation," *High Voltage*, vol. 8, no. 2, pp. 231–238, Apr. 2023, doi: [10.1049/hve2.12253](https://doi.org/10.1049/hve2.12253).
- [19] A. Xu, S. Roland, and X. Colin, "Thermal ageing of a silane-crosslinked polyethylene stabilised with a thiodipropionate antioxidant," *Polym. Degradation Stability*, vol. 181, Nov. 2020, Art. no. 109276, doi: [10.1016/j.polymdegradstab.2020.109276](https://doi.org/10.1016/j.polymdegradstab.2020.109276).
- [20] A. Xu, S. Roland, and X. Colin, "Physico-chemical characterization of the blooming of Irganox 1076® antioxidant onto the surface of a silane-crosslinked polyethylene," *Polym. Degradation Stability*, vol. 171, Jan. 2020, Art. no. 109046, doi: [10.1016/j.polymdegradstab.2019.109046](https://doi.org/10.1016/j.polymdegradstab.2019.109046).
- [21] S. V. Suraci and D. Fabiani, "Quantitative investigation and modelling of the electrical response of XLPE insulation with different filler content," in *Proc. IEEE Conf. Electr. Insul. Dielectric Phenomena (CEIDP)*, Oct. 2020, pp. 439–442, doi: [10.1109/CEIDP49254.2020.9437470](https://doi.org/10.1109/CEIDP49254.2020.9437470).

- [22] S. Liu, S. W. Veysey, L. S. Fifield, and N. Bowler, "Quantitative analysis of changes in antioxidant in crosslinked polyethylene (XLPE) cable insulation material exposed to heat and gamma radiation," *Polym. Degradation Stability*, vol. 156, pp. 252–258, Oct. 2018, doi: [10.1016/j.polymdegradstab.2018.09.011](https://doi.org/10.1016/j.polymdegradstab.2018.09.011).
- [23] T. T. N. Vu, G. Teyssedre, B. Vissouvanadin, S. L. Roy, and C. Laurent, "Correlating conductivity and space charge measurements in multi-dielectrics under various electrical and thermal stresses," *IEEE Trans. Dielectr. Electr. Insul.*, vol. 22, no. 1, pp. 117–127, Feb. 2015, doi: [10.1109/TDEI.2014.004507](https://doi.org/10.1109/TDEI.2014.004507).
- [24] E. Mustafa, R. S. A. Afia, O. Nouini, and Z. Á. Tamus, "Implementation of non-destructive electrical condition monitoring techniques on low-voltage nuclear cables: I. Irradiation aging of EPR/CSPE cables," *Energies*, vol. 14, no. 16, p. 5139, Aug. 2021, doi: [10.3390/en14165139](https://doi.org/10.3390/en14165139).
- [25] F. Kremer and A. Schönhal, *Broadband Dielectric Spectroscopy*. Berlin, Germany: Springer, 2003, doi: [10.1007/978-3-642-56120-7](https://doi.org/10.1007/978-3-642-56120-7).
- [26] V. M. Gun'ko, V. I. Zarko, E. V. Goncharuk, L. S. Andriyko, V. V. Turov, Y. M. Nychiporuk, R. Lebeda, J. Skubiszewska-Zięba, A. L. Gabchak, V. D. Osovskii, Y. G. Ptushinskii, G. R. Yurchenko, O. A. Mishchuk, P. P. Gorbik, P. Pissis, and J. P. Blitz, "TSDC spectroscopy of relaxational and interfacial phenomena," *Adv. Colloid Interface Sci.*, vol. 131, nos. 1–2, pp. 1–89, Feb. 2007, doi: [10.1016/j.cis.2006.11.001](https://doi.org/10.1016/j.cis.2006.11.001).
- [27] G. Teyssedre, F. Zheng, L. Boudou, and C. Laurent, "Charge trap spectroscopy in polymer dielectrics: A critical review," *J. Phys. D, Appl. Phys.*, vol. 54, no. 26, Apr. 2021, Art. no. 263001, doi: [10.1088/1361-6463/abf44a](https://doi.org/10.1088/1361-6463/abf44a).
- [28] T. Mizutani, Y. Suzuoki, M. Hanai, and M. Ieda, "Determination of trapping parameters from TSC in polyethylene," *Jpn. J. Appl. Phys.*, vol. 21, no. 11R, p. 1639, Nov. 1982, doi: [10.1143/JJAP.21.1639](https://doi.org/10.1143/JJAP.21.1639).
- [29] F. Tian, W. Bu, L. Shi, C. Yang, Y. Wang, and Q. Lei, "Theory of modified thermally stimulated current and direct determination of trap level distribution," *J. Electrostatics*, vol. 69, no. 1, pp. 7–10, Feb. 2011, doi: [10.1016/j.elstat.2010.10.001](https://doi.org/10.1016/j.elstat.2010.10.001).
- [30] S. Diahham, P. Lambkin, and B. Chen, "Nonlinear dielectric properties of polyimide in high AC electric field," *J. Appl. Phys.*, vol. 132, no. 15, Oct. 2022, Art. no. 154101, doi: [10.1063/5.0108674](https://doi.org/10.1063/5.0108674).
- [31] S. V. Suraci, D. Fabiani, S. Roland, and X. Colin, "Multi scale aging assessment of low-voltage cables subjected to radio-chemical aging: Towards an electrical diagnostic technique," *Polym. Test.*, vol. 103, Nov. 2021, Art. no. 107352, doi: [10.1016/j.polymertesting.2021.107352](https://doi.org/10.1016/j.polymertesting.2021.107352).
- [32] L. Chen, T. D. Huan, and R. Ramprasad, "Electronic structure of polyethylene: Role of chemical, morphological and interfacial complexity," *Sci. Rep.*, vol. 7, no. 1, p. 6128, Jul. 2017, doi: [10.1038/s41598-017-06357-y](https://doi.org/10.1038/s41598-017-06357-y).
- [33] H. Uehara, T. Okamoto, Y. Sekii, S. Iwata, and T. Takada, "Analysis of charge trap depth using Q(t) method and quantum chemical calculation in XLPE and PE with phenolic antioxidant," in *Proc. IEEE Conf. Electr. Insul. Dielectric Phenomena (CEIDP)*, Dec. 2021, pp. 454–457, doi: [10.1109/CEIDP50766.2021.9705439](https://doi.org/10.1109/CEIDP50766.2021.9705439).
- [34] S. V. Suraci and D. Fabiani, "Aging modeling of low-voltage cables subjected to radio-chemical aging," *IEEE Access*, vol. 9, pp. 83569–83578, 2021, doi: [10.1109/ACCESS.2021.3086987](https://doi.org/10.1109/ACCESS.2021.3086987).
- [35] S. V. Suraci, D. Fabiani, A. Xu, S. Roland, and X. Colin, "Ageing assessment of XLPE LV cables for nuclear applications through physico-chemical and electrical measurements," *IEEE Access*, vol. 8, pp. 27086–27096, 2020, doi: [10.1109/ACCESS.2020.2970833](https://doi.org/10.1109/ACCESS.2020.2970833).
- [36] A. Xu, S. Roland, and X. Colin, "Physico-chemical analysis of a silane-grafted polyethylene stabilised with an excess of Irganox 1076<sup>®</sup>. Proposal of a microstructural model," *Polym. Degradation Stability*, vol. 183, Jan. 2021, Art. no. 109453, doi: [10.1016/j.polymdegradstab.2020.109453](https://doi.org/10.1016/j.polymdegradstab.2020.109453).
- [37] D. K. Das-Gupta, "Polyethylene: Structure, morphology, molecular motion and dielectric behavior," *IEEE Elect. Insul. Mag.*, vol. 10, no. 3, pp. 5–15, May 1994.
- [38] E. Logakis, L. Petersson, and J. Viertel, "Dielectric spectroscopy and thermally stimulated depolarization current investigations in low density polyethylene," in *Proc. IEEE Int. Conf. Solid Dielectr. (ICSD)*, Jun. 2013, pp. 948–951.
- [39] P. Frübing, D. Blischke, R. Gerhard-Multhaupt, and M. S. Khalil, "Complete relaxation map of polyethylene: Filler-induced chemical modifications as dielectric probes," *J. Phys. D, Appl. Phys.*, vol. 34, no. 20, p. 3051, 2001.
- [40] H. Uehara, T. Okamoto, Y. Sekii, S. Iwata, and T. Takada, "Electric field and temperature characteristics of accumulated charge amount in several polymeric insulating materials using Q(t) method and quantum chemical calculation," in *Proc. IEEE Conf. Electr. Insul. Dielectric Phenomena (CEIDP)*, Oct. 2022, pp. 13–16, doi: [10.1109/CEIDP55452.2022.9985349](https://doi.org/10.1109/CEIDP55452.2022.9985349).
- [41] S. Serra, E. Tosatti, S. Iarlori, S. Scandolo, and G. Santoro, "Interchain electron states in polyethylene," *Phys. Rev. B, Condens. Matter*, vol. 62, no. 7, pp. 4389–4393, Aug. 2000, doi: [10.1103/PhysRevB.62.4389](https://doi.org/10.1103/PhysRevB.62.4389).



**SIMONE VINCENZO SURACI** (Member, IEEE) received the B.Sc. degree in civil and environmental engineering from the University of Reggio Calabria, in 2015, the M.Sc. degree in energy and nuclear engineering from the University of Bologna, in 2017, and the Ph.D. degree in electrical engineering and polymer science from the University of Bologna and the Arts et Métiers Institute of Technology, Paris, in 2020. He is currently an Assistant Professor with the Department of Electrical Electronics and Information Engineering, University of Bologna. His research interests include the study of polymeric dielectrics for nuclear and HVDC applications and their degradation with aging, nondestructive diagnosis techniques for insulation materials, and nano-structured composites. He has been a member of DEIS, since 2017.



**DANIELE MARIANI** (Graduate Student Member, IEEE) received the B.Sc. and master's degrees in electrical engineering from the University of Bologna, Italy, in 2018 and 2021, respectively, where he is currently pursuing the Ph.D. degree. His work includes the incorporation of semi-conductive quantum dots in epoxy resins and data analysis of experimental outcomes, which comprises space charge, conductivity, and dielectric spectroscopy measurements. His main current research interest includes the electrical characterization of polymeric materials and their nanocomposites.



**DAVIDE FABIANI** (Senior Member, IEEE) is currently an Associate Professor of innovative electrical technologies and design and diagnostics of electrical insulation with the Department of Electrical Electronics and Information Engineering, University of Bologna. He is the coauthor of about 220 papers, most of them published on the major international journals and conference proceedings. His research interests include the development, characterization and diagnosis of electrical insulation systems for applications in electrical and electronic apparatus. He is an Associate Editor of *IET High Voltage* and the VP Admin of IEEE DEIS 2023.